Light-Meson Spectroscopy at COMPASS

18^{th} International Workshop on Meson Physics
Kraków, Poland

David Spülbeck
on behalf of the COMPASS Collaboration
spuelbeck@hiskp.uni-bonn.de

27 June 2026

UNIVERSITÄT BONN

MESON 2026

Constituent-Quark Model

- $|q\bar{q}'\rangle$ system with $q = u, d, s$
- Quantum numbers $J^{P(C)}$

Constituent-Quark Model

Light Mesons: $m < 3\,\mathrm{GeV}/c^2$

Constituent-Quark Model

- $|q\bar{q}'\rangle$ system with $q = u, d, s$
- Quantum numbers $J^{P(C)}$

In unflavoured sector: Spin-exotics

- Not possible in Constituent-Quark Model: $J^{PC} = 0^{--}, (odd)^{-+}, (even)^{+-}$
- Access to exotic states that do not overlap with ordinary mesons

Hybrids

- Excited gluonic field contributes to J^{PC}
- Predictions from theory: lightest hybrids have $J^{PC} = (0, \mathbf{1}, 2)^{-(+)}, 1^{-(-)}$

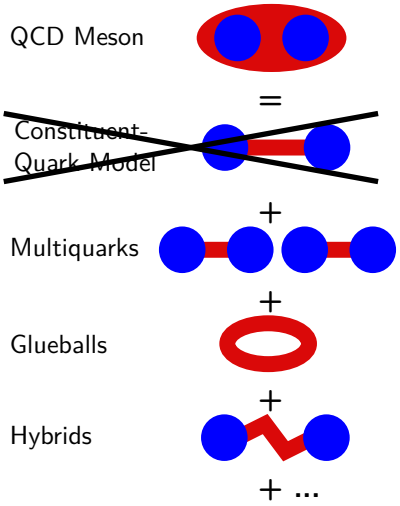

- **CO**mmon **M**uon **P**roton **A**pparatus for **S**tructure and **S**pectroscopy
- Located at the M2 beam line in the north area of CERN
- Part of the Hadron program: Light-Meson Spectroscopy

Setup for Hadron beams

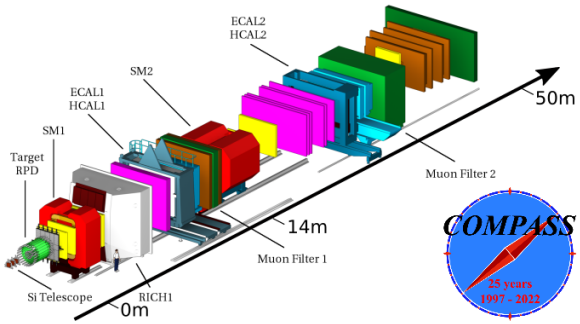

Diffractive resonance production

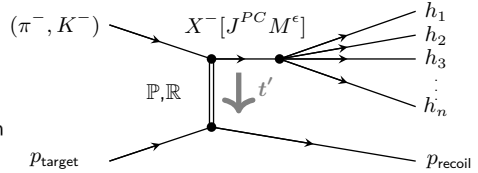

- Beam hadrons at $190\,\text{GeV}/c$
  $\rightarrow$ mainly Pomeron exchange
- Diff. cross section:

$$\frac{\mathrm{d}\sigma_{\pi+p\to X+p}}{\mathrm{d}m_X\,\mathrm{d}t'\,\mathrm{d}\phi(m_X,\tau_n)} \propto m_X \left|\mathcal{M}_{fi}(m_X,t',\tau_n)\right|^2$$

Analysis in two steps:

1. Partial-Wave Decomposition (PWD): Amplitudes of contributing waves are determined
2. Resonance-Model Fit (RMF): Extraction of resonance parameters (m_0, Γ_0) and couplings

$$\mathcal{M}_{fi}\left(m_X, t', \tau_n\right) = \mathcal{P}\left(m_X, t'\right) \sum_{a}^{N_{\text{waves}}} \left[\sum_{k \in \mathbb{S}_a} \mathcal{C}_{ka}\left(t'\right) \mathcal{D}_k\left(m_X\right) \right] \Psi_a\left(m_X, \tau_n\right)$$

Partial-Wave Analysis for diffractive production

Analysis in two steps:

1. Partial-Wave Decomposition (PWD): Amplitudes of contributing waves are determined
2. Resonance-Model Fit (RMF): Extraction of resonance parameters (m_0, Γ_0) and couplings

$$\mathcal{M}_{fi}\left(m_X, t', \tau_n\right) = \underbrace{\mathcal{P}\left(m_X, t'\right) \sum_a^{N_\text{waves}} \left[\sum_{k \in \mathbb{S}_a} \mathcal{C}_{ka}\left(t'\right) \mathcal{D}_k\left(m_X\right) \right]}_{\mathcal{T}_a} \Psi_a\left(m_X, \tau_n\right)$$

Partial-Wave Decomposition

- Data arranged into bins of (m_X, t')

$$\mathcal{I}(\tau) = \left| \sum_a^{N_\text{waves}} \mathcal{T}_a \Psi_a(\tau) \right|^2$$

- Decay Amplitudes Ψ_a are calculated from data using isobar model
- Production amplitudes $\mathcal{T}_a$ are determined in extended Likelihood fit

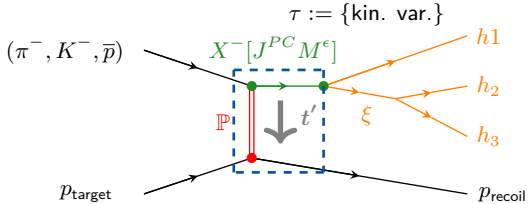

Partial wave: $J^{PC}M^\epsilon\xi_1\xi_2 LS$; ξ – decay
(Diffractive resonance production and subsequent two-body decays)

Example: PWD of $\pi^-\pi^+\pi^-\eta$

Decomposition into decay channels

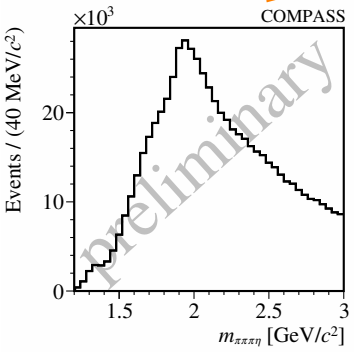

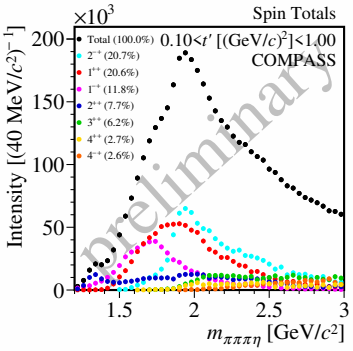

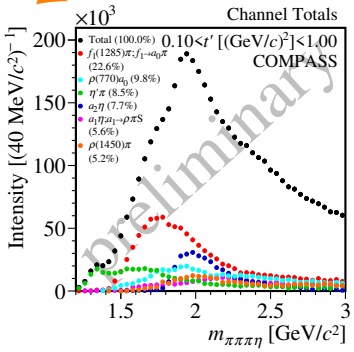

Decomposition into J^{PC}

Analysis in two steps:

1. Partial-Wave Decomposition (PWD): Amplitudes of contributing waves are determined
2. Resonance-Model Fit (RMF): Extraction of resonance parameters (m_0, Γ_0) and couplings

$$\mathcal{T}_a(m_X, t') \propto \mathcal{P}\left(m_X, t'\right) \sum_{k \in \mathbb{S}_a} \mathcal{C}_{ka}\left(t'\right) \mathcal{D}_k\left(m_X\right)$$

SDM: $\rho_{ab}(m_X, t') = \mathcal{T}_a(m_X, t')\mathcal{T}_b^*(m_X, t')$

Resonance-Model Fit

- Measured amplitudes are modelled by sum of resonant and non-resonant components ($\mathbb{S}$)
- Dynamics of resonant components:
  $\mathcal{D}_{\text{res.}}(m_X) = \frac{m_0\Gamma_0}{m_X^2 - m_0^2 - im_0\Gamma(m_X)}$
- Dynamics of non-resonant component per partial wave i:
  $\mathcal{D}^i_{\text{n-res.}}(m_X) = (m_X - m_{\text{Thr}})^{a_i} \exp\left[-b\tilde{q}_i^2(m_X)\right]$
- Perform χ^2 fit

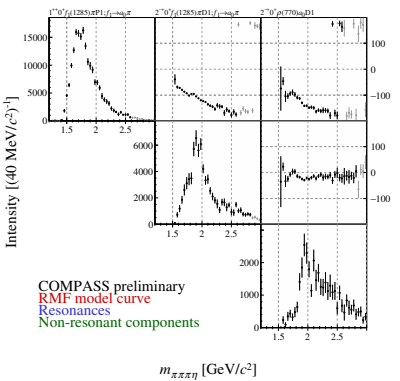

Analysis in two steps:

1. Partial-Wave Decomposition (PWD): Amplitudes of contributing waves are determined
2. Resonance-Model Fit (RMF): Extraction of resonance parameters (m_0, Γ_0) and couplings

$$\mathcal{T}_a(m_X, t') \propto \mathcal{P}\left(m_X, t'\right) \sum_{k \in \mathbb{S}_a} \mathcal{C}_{ka}\left(t'\right) \mathcal{D}_k\left(m_X\right)$$

SDM: $\rho_{ab}(m_X, t') = \mathcal{T}_a(m_X, t')\mathcal{T}_b^*(m_X, t')$

Resonance-Model Fit

- Measured amplitudes are modelled by sum of resonant and non-resonant components ($\mathbb{S}$)
- Dynamics of resonant components:
  $\mathcal{D}_{\text{res.}}(m_X) = \frac{m_0\Gamma_0}{m_X^2 - m_0^2 - im_0\Gamma(m_X)}$
- Dynamics of non-resonant component per partial wave i:
  $\mathcal{D}^i_{\text{n-res.}}(m_X) = (m_X - m_{\text{Thr}})^{a_i} \exp\left[-b\tilde{q}_i^2(m_X)\right]$
- Perform χ^2 fit

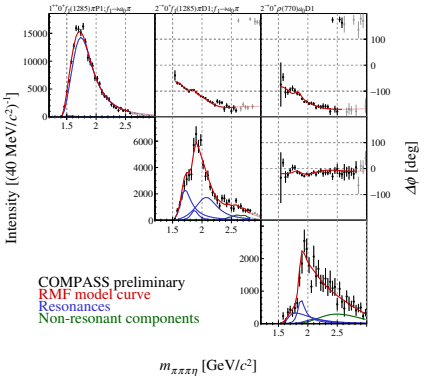

Analysis in two steps:

1. Partial-Wave Decomposition (PWD): Amplitudes of contributing waves are determined
2. Resonance-Model Fit (RMF): Extraction of resonance parameters (m_0, Γ_0) and couplings

$$\mathcal{T}_a(m_X, t') \propto \mathcal{P}\left(m_X, t'\right) \sum_{k \in \mathbb{S}_a} \mathcal{C}_{ka}\left(t'\right) \mathcal{D}_k\left(m_X\right)$$

SDM: $\rho_{ab}(m_X, t') = \mathcal{T}_a(m_X, t')\mathcal{T}_b^*(m_X, t')$

Resonance-Model Fit

- Measured amplitudes are modelled by sum of resonant and non-resonant components ($\mathbb{S}$)
- Dynamics of resonant components:
  $\mathcal{D}_{\text{res.}}(m_X) = \frac{m_0\Gamma_0}{m_X^2 - m_0^2 - im_0\Gamma(m_X)}$
- Dynamics of non-resonant component per partial wave i:
  $\mathcal{D}^i_{\text{n-res.}}(m_X) = (m_X - m_{\text{Thr}})^{a_i} \exp\left[-b\tilde{q}_i^2(m_X)\right]$
- Perform χ^2 fit

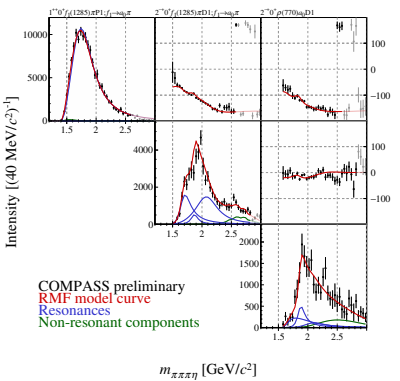

$a_J \to K^0_S K^-$ - 430 k events

- Reaction: $\pi^- + p \to K^- K^0_S(\pi^+\pi^-) + p$
- 6 resonances in 4 waves simultaneously

$(\pi_J/a_J) \to \pi^-\pi^-\pi^+\eta$ - 630 k events

- Reaction: $\pi^- + p \to \pi^-\pi^-\pi^+\eta + p$, $\eta \to \gamma\gamma$
- 11 resonances in 17 waves simultaneously

$(\pi_J/a_J) \to \omega\pi^-\pi^0$ - 720 k events

- Reaction: $\pi^- + p \to \omega\pi^-\pi^0 + p$, $\omega \to \pi^+\pi^-\pi^0$, $\pi^0 \to \gamma\gamma$
- 11 resonance in 23 waves simultaneously

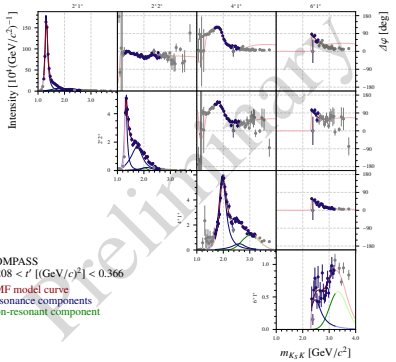

- No isobars
- Ambiguities are challenging

$a_J \to K_S^0 K^-$ - 430 k events

- Reaction: $\pi^- + p \to K^- K_S^0(\pi^+\pi^-) + p$
- 6 resonances in 4 waves simultaneously

$(\pi_J/a_J) \to \pi^-\pi^-\pi^+\eta$ - 630 k events

- Reaction: $\pi^- + p \to \pi^-\pi^-\pi^+\eta + p$, $\eta \to \gamma\gamma$
- 11 resonances in 17 waves simultaneously

$(\pi_J/a_J) \to \omega\pi^-\pi^0$ - 720 k events

- Reaction: $\pi^- + p \to \omega\pi^-\pi^0 + p$, $\omega \to \pi^+\pi^-\pi^0$, $\pi^0 \to \gamma\gamma$
- 11 resonance in 23 waves simultaneously

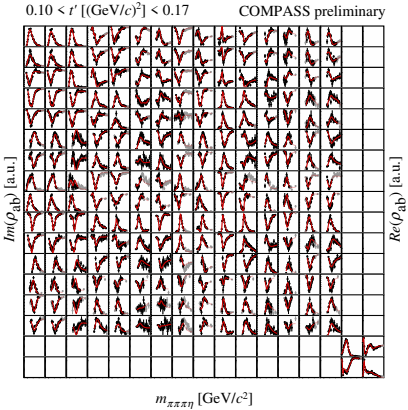

- Main isobars: $f_1(1285), \rho(770), a_0(980), \eta', a_2(1320)$

Latest analyses

$a_J \to K_S^0 K^-$ - 430 k events

- Reaction: $\pi^- + p \to K^- K_S^0(\pi^+\pi^-) + p$
- 6 resonances in 4 waves simultaneously

$(\pi_J/a_J) \to \pi^-\pi^-\pi^+\eta$ - 630 k events

- Reaction: $\pi^- + p \to \pi^-\pi^-\pi^+\eta + p$, $\eta \to \gamma\gamma$
- 11 resonances in 17 waves simultaneously

$(\pi_J/a_J) \to \omega\pi^-\pi^0$ - 720 k events

- Reaction: $\pi^- + p \to \omega\pi^-\pi^0 + p$, $\omega \to \pi^+\pi^-\pi^0$, $\pi^0 \to \gamma\gamma$
- 11 resonance in 23 waves simultaneously

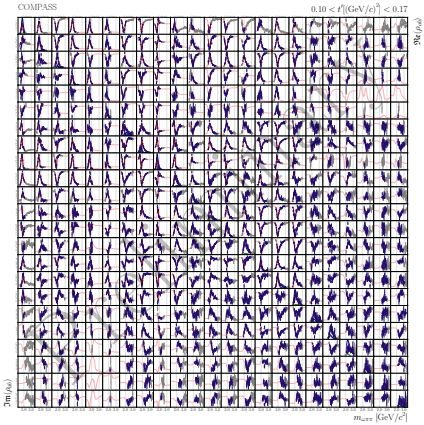

- Main isobars: $b_1(1235)$, $\rho(770)$, $\rho_3(1690)$

$K_S^0 K^-$

- Dominant $a_2(1320)$
- $a_2(1320)$ & $a_2(1700)$ consistent with previous measurements
- Higher a_2 above $2.0\,\mathrm{GeV}/c^2$

		$K_S^0 K^-$
$a_2(1320)$	m_0	$1316.63 \pm 0.20^{+2.23}_{-2.33}$
	Γ_0	$109.5 \pm 0.4^{+2.6}_{-2.0}$
$a_2(1700)$	m_0	$1748 \pm 4^{+13}_{-86}$
	Γ_0	$534 \pm 9^{+26}_{-230}$
$a_2(2030)$	m_0	$2124 \pm 5^{+37}_{-9}$
	Γ_0	$527 \pm 13^{+55}_{-250}$

(in MeV/c^2)

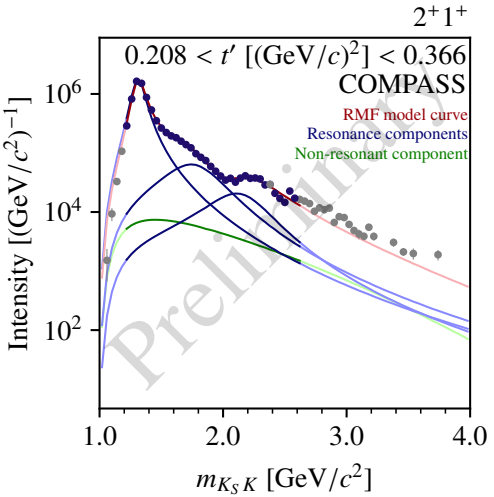

$\pi^-\pi^-\pi^+\eta$

- 3 decay channels: $\eta'\pi$, $f_1(1285)\pi$, $a_2(1320)\eta$
- $a_2(1320)$ & $a_2(1700)$ consistent with previous measurements
- Higher a_2 above $2.0\,\mathrm{GeV}/c^2$

		$K^0_S K^-$	$\pi^-\pi^-\pi^+\eta$
$a_2(1320)$	m_0	$1316.63 \pm 0.20^{+2.23}_{-2.33}$	$1315.0 \pm 1.1^{+2.3}_{-10.1}$
	Γ_0	$109.5 \pm 0.4^{+2.6}_{-2.0}$	$108.2 \pm 2.5^{+10.1}_{-5.0}$
$a_2(1700)$	m_0	$1748 \pm 4^{+13}_{-86}$	$1752 \pm 10^{+16}_{-21}$
	Γ_0	$534 \pm 9^{+26}_{-230}$	$485 \pm 27^{+11}_{-63}$
$a_2(2030)$	m_0	$2124 \pm 5^{+37}_{-9}$	$2054 \pm 6^{+95}_{-16}$
	Γ_0	$527 \pm 13^{+55}_{-250}$	$351 \pm 15^{+87}_{-0}$

(in MeV/c^2)

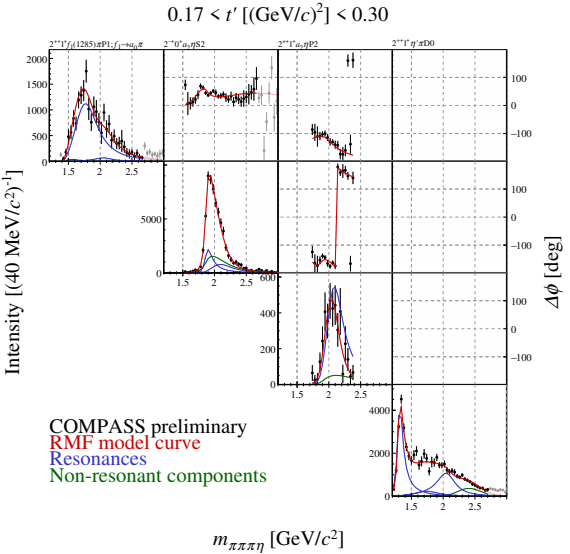

First Lattice QCD calculations

- Decay of hybrid meson with $J^{PC} = 1^{-+}$ via several channels
- At $\mathcal{SU}(3)$ symmetry point:
  - $\rightarrow$ $m_{u,d,s} = m_s^{exp.}$
  - $\rightarrow$ $m_\pi \approx 700\,\mathrm{MeV/c^2}$
  - $\rightarrow$ $3m_\pi$ pushed to high energy
- Result: $b_1\pi$ most dominant

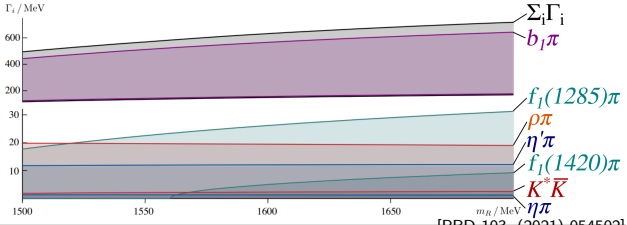

[PRD 103, (2021) 054502]

First Lattice QCD calculations

- Decay of hybrid meson with $J^{PC} = 1^{-+}$ via several channels
- At $\mathcal{SU}(3)$ symmetry point:
  - $\rightarrow$ $m_{u,d,s} = m_s^{exp.}$
  - $\rightarrow$ $m_\pi \approx 700\,\mathrm{MeV/c^2}$
  - $\rightarrow$ $3m_\pi$ pushed to high energy
- Result: $b_1\pi$ most dominant

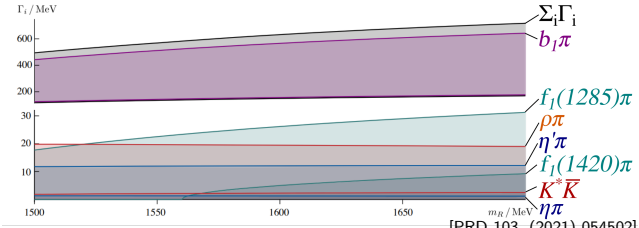

[PRD 103, (2021) 054502]

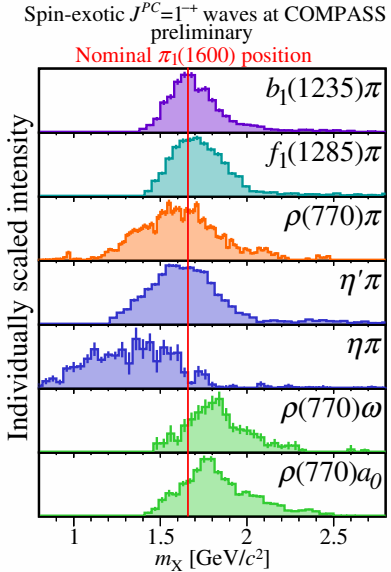

$\omega\pi^-\pi^0$

- 2 decay channels:
  $b_1(1235)\pi$& $\rho(770)\omega$
- $b_1(1235)\pi$ is dominant
- $\rho(770)\omega$ is significant

	$\omega\pi\pi$	$\pi^-\pi^-\pi^+\eta$	$\pi^-\pi^+\pi$
m_0	$1723 \pm 6^{+37}_{-14}$	$1706.2 \pm 2.6^{+7.0}_{-56.2}$	1600^{+110}_{-60}
Γ_0	$336 \pm 10^{+96}_{-33}$	$377 \pm 5^{+17}_{-11}$	580^{-100}_{-230}

(in MeV/c^2)

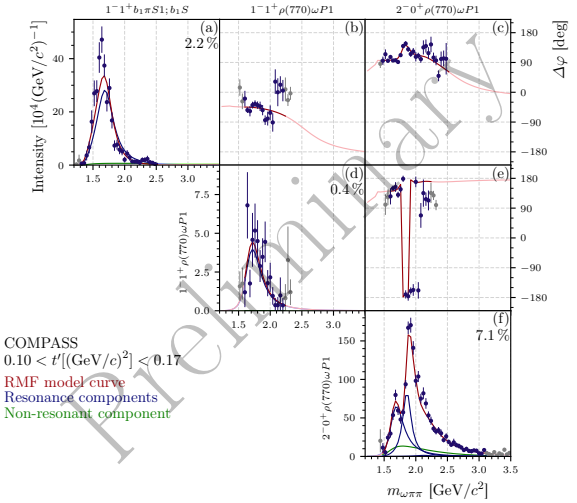

$\pi^-\pi^-\pi^+\eta$

- 3 decay channels:
  $f_1(1285)\pi$, $\rho(770)a_0$, $\eta'\pi$
- $f_1(1285)\pi$ and $\eta'\pi$ are dominant
- $\rho(770)a_0$ is significant

$$\frac{\Gamma^{\pi_1(1600)}_{f_1(1285)\pi}}{\Gamma^{\pi_1(1600)}_{\eta'\pi}} = 1.014 \underbrace{\pm 0.034}_{\text{stat.}} \underbrace{{}^{+0.171}_{-0.044}}_{\text{sys.}} \underbrace{\pm 0.11}_{\text{PDG}}$$

	$\omega\pi\pi$	$\pi^-\pi^-\pi^+\eta$	$\pi^-\pi^+\pi$
m_0	$1723 \pm 6^{+37}_{-14}$	$1706.2 \pm 2.6^{+7.0}_{-56.2}$	1600^{+110}_{-60}
Γ_0	$336 \pm 10^{+96}_{-33}$	$377 \pm 5^{+17}_{-11}$	580^{-100}_{-230}

(in MeV/c^2)

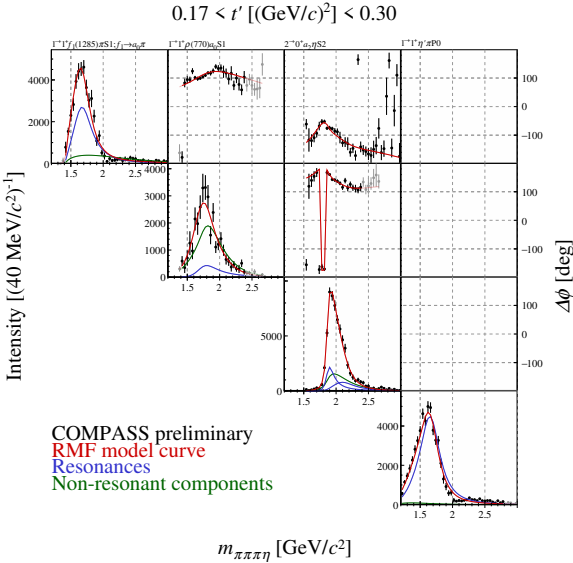

$\pi^-\pi^-\pi^+\eta$

- 3 decay channels:
  $f_1(1285)\pi$, $\rho(770)a_0$, $\eta'\pi$
- $f_1(1285)\pi$ and $\eta'\pi$ are dominant
- $\rho(770)a_0$ is significant
- $$\frac{\Gamma^{\pi_1(1600)}_{f_1(1285)\pi}}{\Gamma^{\pi_1(1600)}_{\eta'\pi}} = 1.014 \underbrace{\pm 0.034}_{\text{stat.}} \underbrace{^{+0.171}_{-0.044}}_{\text{sys.}} \underbrace{\pm 0.11}_{\text{PDG}}$$

	$\omega\pi\pi$	$\pi^-\pi^-\pi^+\eta$	$\pi^-\pi^+\pi$
m_0	$1723 \pm 6^{+37}_{-14}$	$1706.2 \pm 2.6^{+7.0}_{-56.2}$	1600^{+110}_{-60}
Γ_0	$336 \pm 10^{+96}_{-33}$	$377 \pm 5^{+17}_{-11}$	580^{-100}_{-230}

(in MeV/c^2)

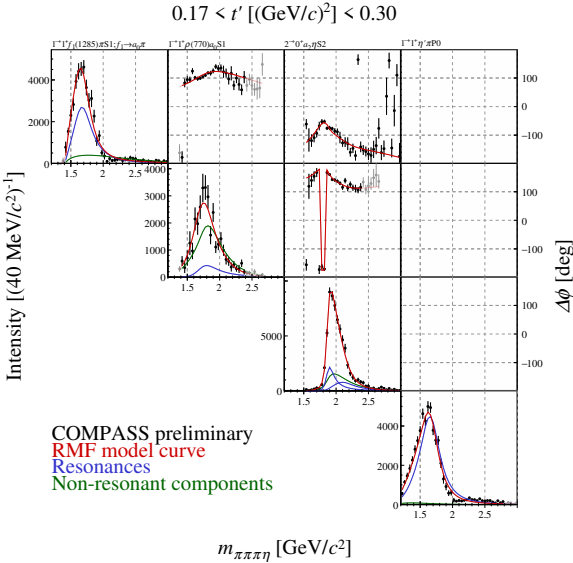

COMPASS results: Overview

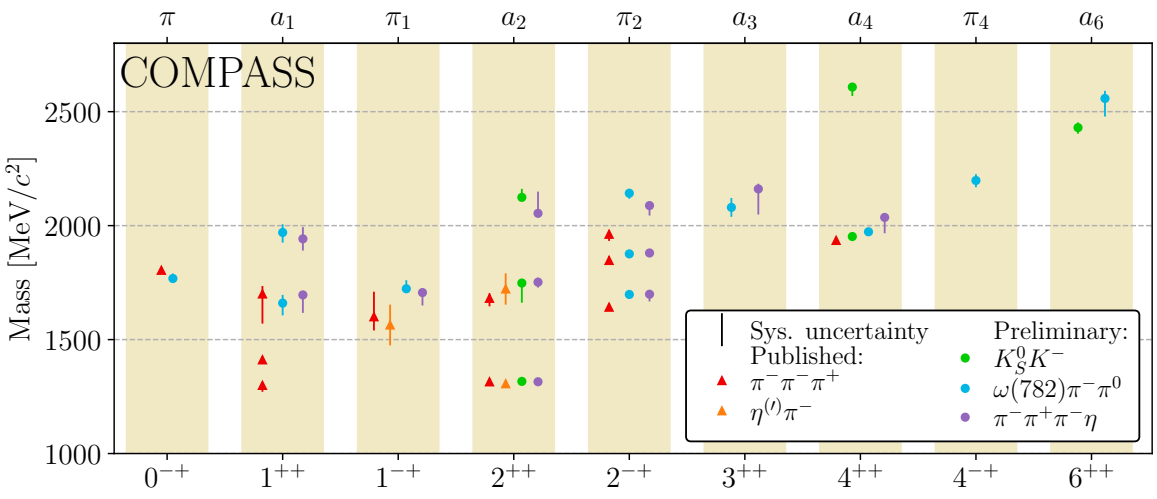

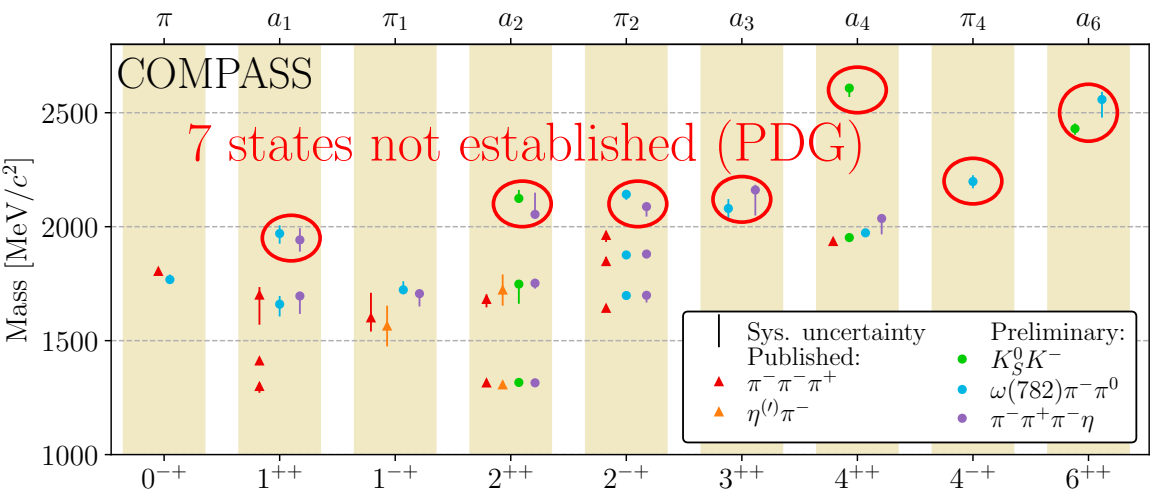
COMPASS
7 states not established (PDG)
Mass [MeV/c^2]
2500
2000
1500
1000
π a_1 π_1 a_2 π_2 a_3 a_4 π_4 a_6
0^{-+} 1^{++} 1^{-+} 2^{++} 2^{-+} 3^{++} 4^{++} 4^{-+} 6^{++}
Sys. uncertainty
Published:
$\pi^-\pi^-\pi^+$
$\eta^{(\prime)}\pi^-$
Preliminary:
$K^0_S K^-$
$\omega(782)\pi^-\pi^0$
$\pi^-\pi^+\pi^-\eta$

COMPASS: Data

- $K^- + p \to K^-\pi^+\pi^- + p$ at $190\,\mathrm{GeV/c}$
- $720\,\mathrm{k}$ events
- Four t'-bins in range $0.1 < t' < 1.0\,(\mathrm{GeV/c})^2$
- Limited by PID in spectrometer

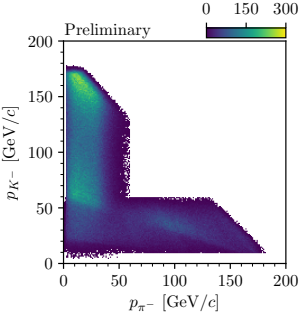

COMPASS: Resonance-Model Fit

- Agreement with at least five established states
- Agreement with at least three not established states

PDG: Light Strange Sector

- 25 states listed, nine need further confirmation

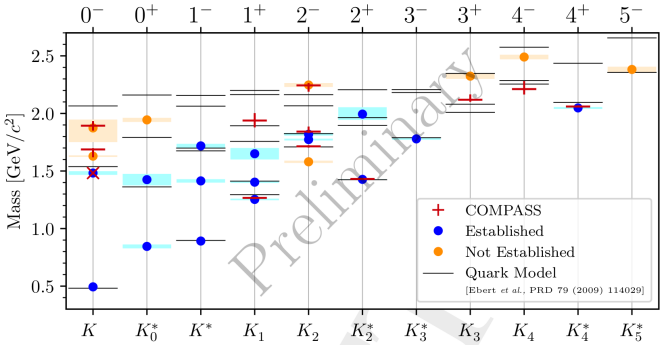

COMPASS: Data

- $K^- + p \to K^-\pi^+\pi^- + p$ at 190 GeV/c
- 720 k events
- Four t'-bins in range $0.1 < t' < 1.0\,(\mathrm{GeV/c})^2$
- Limited by PID in spectrometer

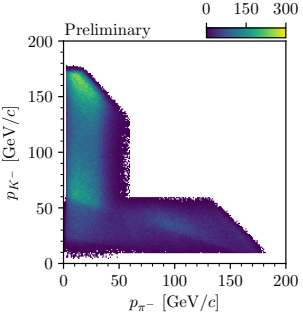

Exotic state in 0^- sector?

- Constituent-Quark Model predicts two excited states
- Three exited signals are observed

PDG: Light Strange Sector

- 25 states listed, nine need further confirmation

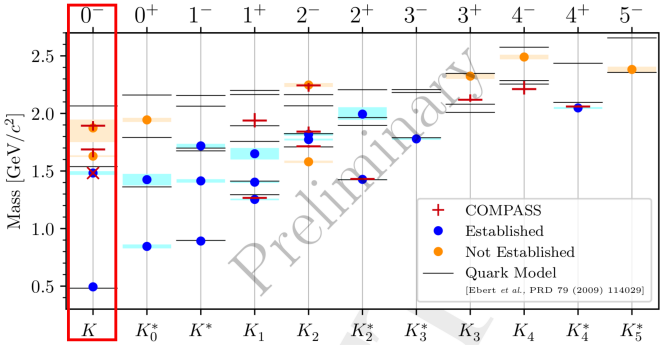

Exotic state in 0^- sector?

$K^-\pi^-\pi^+$

- One decay channels $\rho(770)K^-$
- Real and imaginary parts drive the fit
- Crypto-exotic $K(1630)$ with significance of 8σ

Resonance	Par.	$K^-\pi^-\pi^+$
$K(1460)$	m_0	1482.4 (fixed)
	Γ_0	335.6 (fixed)
$K(1630)$	m_0	$1687 \pm 10^{+2}_{-67}$
	Γ_0	$140 \pm 20^{+50}_{-50}$
$K(1830)$	m_0	$1893 \pm 17^{+13}_{-39}$
	Γ_0	$160 \pm 40^{+60}_{-80}$

(in MeV/c^2)

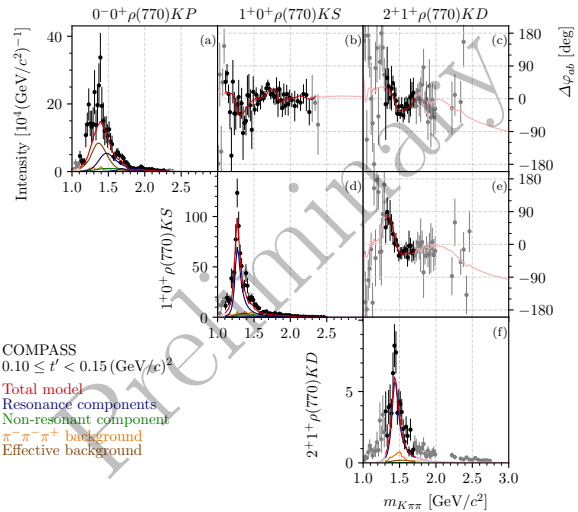

Double Regge processes in $\eta'\pi$

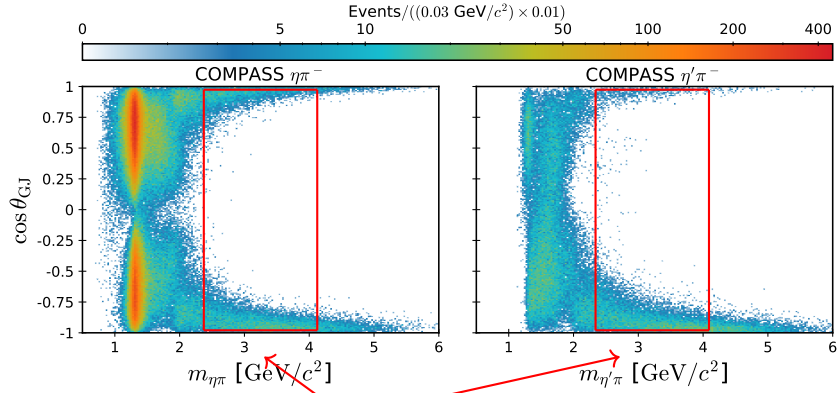

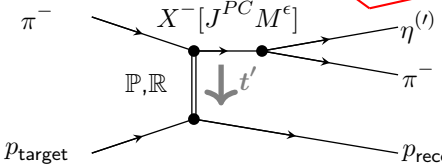

Double Regge processes in $\eta'\pi$

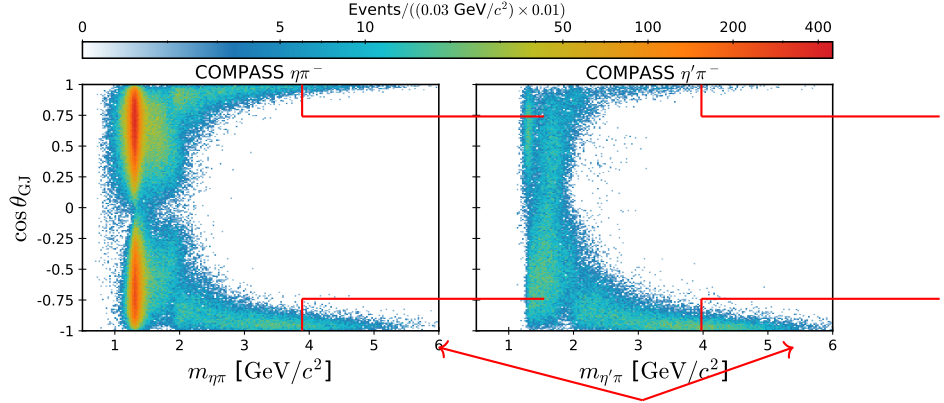

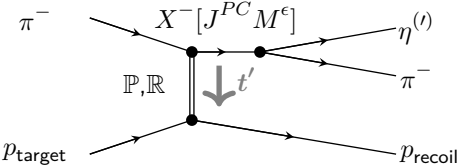

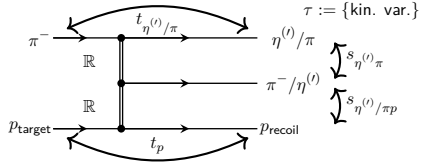

- s-channel resonances with same isospin, intrinsic spin and parity fall on a straight line in the plane: $t = M^2$ vs $\alpha(t) = J$
- The resummation is called a Regge trajectory: $\alpha(t) = \alpha_0 + \alpha' t$
- Scattering amplitude according to Shimada [T. Shimada et al., Nucl.Phys.B142, 344 (1978)]:

$$\mathcal{A}_{\mathbb{R}_1\mathbb{R}_2}(\tau) = \underbrace{F_1(t_\eta)F_2(t_p)}_{\text{Form factors}}\underbrace{T(\alpha_{\mathbb{R}_1}(t_\eta), \alpha_{\mathbb{R}_2}(t_p); s_{\pi p})}_{\text{Shimada model}}$$

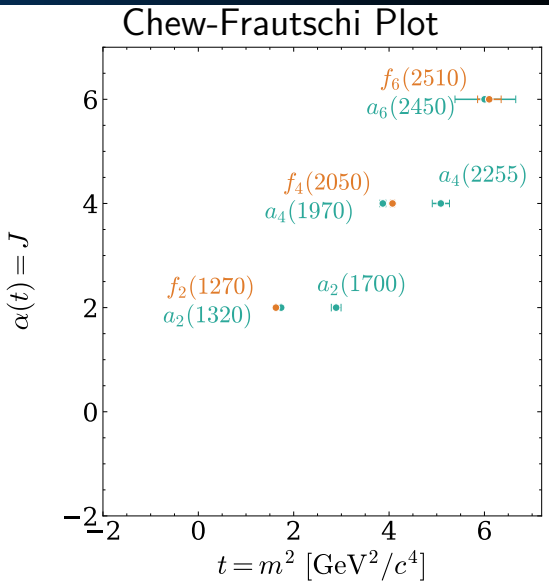

- s-channel resonances with same isospin, intrinsic spin and parity fall on a straight line in the plane: $t = M^2$ vs $\alpha(t) = J$
- The resummation is called a Regge trajectory: $\alpha(t) = \alpha_0 + \alpha' t$
- Scattering amplitude according to Shimada [T. Shimada et al., Nucl.Phys.B142, 344 (1978)]:

$$\mathcal{A}_{\mathbb{R}_1\mathbb{R}_2}(\tau) = \underbrace{F_1(t_\eta)F_2(t_p)}_{\text{Form factors}}\underbrace{T(\alpha_{\mathbb{R}_1}(t_\eta), \alpha_{\mathbb{R}_2}(t_p); s_{\pi p})}_{\text{Shimada model}}$$

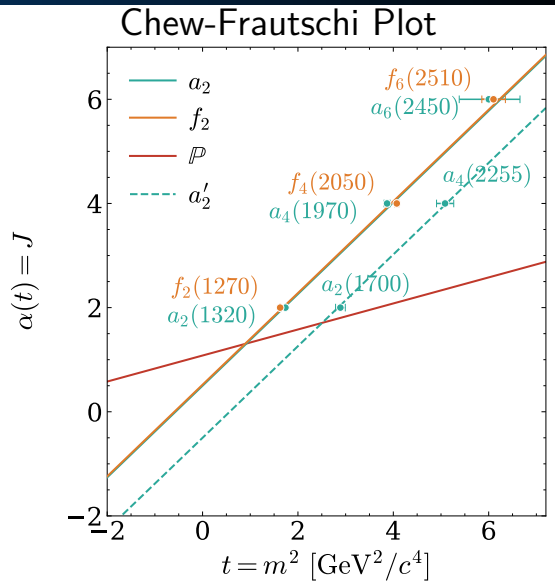

Fit

- Intensity per event k:
  $I_k(\vec{c}, \vec{b}; \tau_k) = \left| \sum c_i \mathcal{A}_i(\vec{b}; \tau_k) \right|^2$
  - c_i are strength
  - b_i are slope parameters of Form factors (t dependence)
- Perform unbinned ext. negative log-likelihood fit
- < 20 parameters needed to fit 23,727 ($\eta\pi^-$) and 21,421 ($\eta'\pi$) events
- First event based fit of double-Regge amplitude
- Compare kinematic distribution: Data (black) vs. weighted MC (red)

Fit

- Intensity per event k:
  $I_k(\vec{c}, \vec{b}; \tau_k) = \left| \sum c_i \mathcal{A}_i(\vec{b}; \tau_k) \right|^2$
  - c_i are strength
  - b_i are slope parameters of Form factors (t dependence)
- Perform unbinned ext. negative log-likelihood fit
- < 20 parameters needed to fit 23,727 $(\eta\pi^-)$ and 21,421 $(\eta'\pi)$ events
- First event based fit of double-Regge amplitude
- Compare kinematic distribution: Data (black) vs. weighted MC (red)

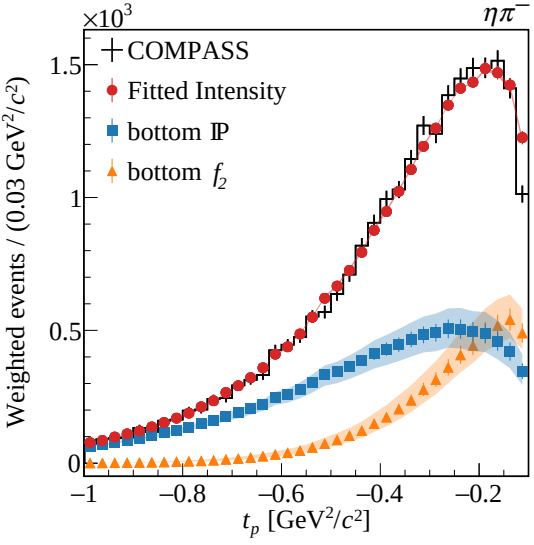

Fitting the double-Regge amplitudes: results

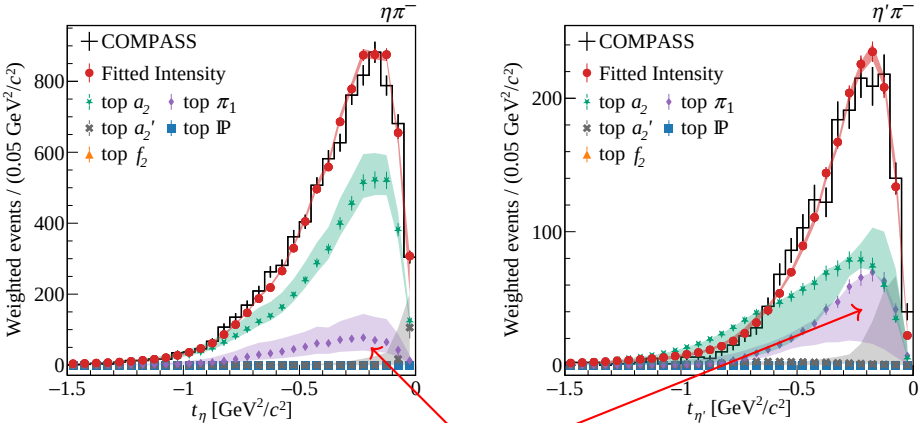

- Significant contribution of exotic π_1 trajectory: 9.9σ $(\eta\pi^-)$ 5.5σ $(\eta'\pi^-)$

Light-meson spectroscopy

- Results from diffractive production with π^-/K^--beam at $190\,\mathrm{GeV}/c$
- Consistent picture of π_J and a_J spectrum from six different final states

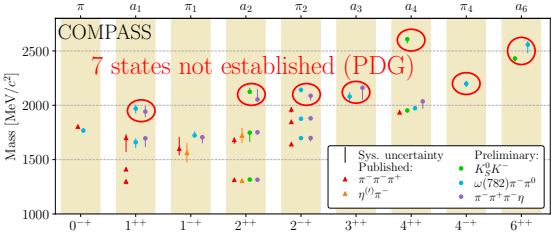

- $\pi_1(1600)$ in seven decay channels
- Observation of crypto-exotic $K(1630)$

Double-Regge Analysis

- First event based fit
- Observation of exotic trajectory π_1

Outlook

- Transition to unitary resonance-model including t'-dependence ..
  - .. for $\eta^{(\prime)}\pi$ (ongoing)
  - .. for multi-body systems
- Use constraints from double-Regge analysis in res. region $(\eta^{(\prime)}\pi)$
- Measuring the strange sector with

AMBER
Apparatus for Meson and Baryon Experimental Research

Back up

More results

$\omega\pi^-\pi^0$

- 2 decay channels:
  $b_1(1235)\pi$& $\rho(770)\omega$
- $\pi_2(1670)$ & $a_2(1880)$ consistent with previous measurements
- Higher π_2 above $2.0\,\mathrm{GeV}/c^2$

		$\omega\pi\pi$
$\pi_2(1670)$	m_0	$1698 \pm 5^{+18}_{-7}$
	Γ_0	$296 \pm 11^{+30}_{-15}$
$\pi_2(1880)$	m_0	$1876 \pm 4^{+4}_{-4}$
	Γ_0	$166 \pm 8^{+8}_{-18}$
$\pi_2(2100)$	m_0	$2142 \pm 12^{+15}_{-21}$
	Γ_0	$304 \pm 21^{+14}_{-34}$

(in MeV/c^2)

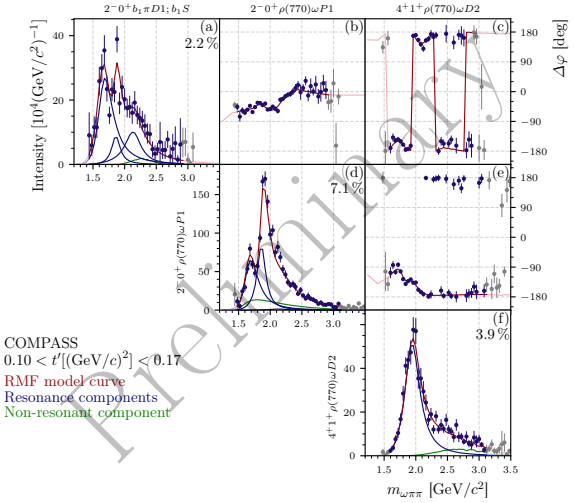

$\pi^-\pi^-\pi^+\eta$

- 3 decay channels:
  $f_1(1285)\pi$, $a_2(1320)\eta$, $\rho(770)a_0(980)$
- $\pi_2(1670)$ & $\pi_2(1880)$ consistent with previous measurements
- Higher π_2 above $2.0\,\mathrm{GeV}/c^2$

		$\omega\pi\pi$	$\pi^-\pi^-\pi^+\eta$
$\pi_2(1670)$	m_0	$1698 \pm 5^{+18}_{-7}$	$1699 \pm 6^{+16}_{-31}$
	Γ_0	$296 \pm 11^{+30}_{-15}$	$223 \pm 11^{+121}_{-8}$
$\pi_2(1880)$	m_0	$1876 \pm 4^{+4}_{-4}$	$1880.0 \pm 3.4^{+3.2}_{-14.1}$
	Γ_0	$166 \pm 8^{+8}_{-18}$	$146 \pm 7^{+16}_{-27}$
$\pi_2(2100)$	m_0	$2142 \pm 12^{+15}_{-21}$	$2088 \pm 8^{+16}_{-43}$
	Γ_0	$304 \pm 21^{+14}_{-34}$	$464 \pm 20^{+34}_{-58}$

(in MeV/c^2)

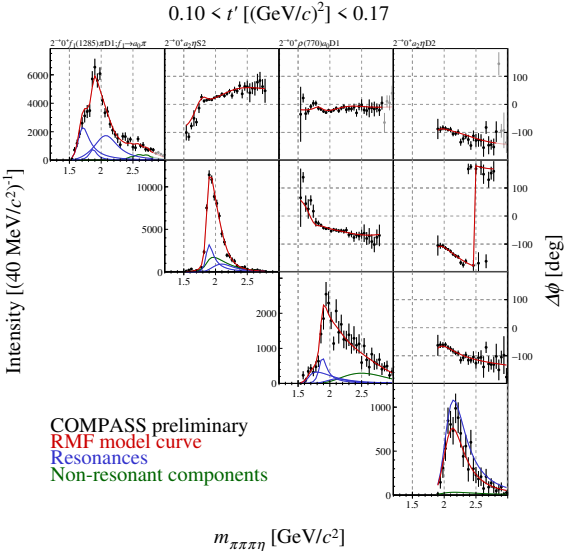

$\omega\pi^-\pi^0$

- 3 decay channels:
  $b_1(1235)\pi$& $\rho(770)\omega$, $\rho_3\pi$
- No a_3 established in PDG

	$\omega\pi\pi$
m_0	$2080 \pm 10^{+40}_{-40}$
Γ_0	$560 \pm 20^{+100}_{-100}$
	(in MeV/c^2)

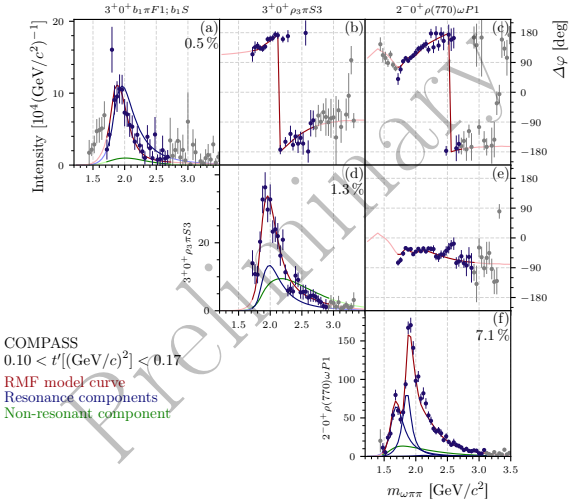

$\pi^-\pi^-\pi^+\eta$

- 3 decay channels:
  $f_1(1285)\pi$, $a_2(1320)\eta$, $\rho(770)a_0(980)$
- No a_3 established in PDG

	$\omega\pi\pi$	$\pi^-\pi^-\pi^+\eta$
m_0	$2080 \pm 10^{+40}_{-40}$	$2161 \pm 6^{+22}_{-112}$
Γ_0	$560 \pm 20^{+100}_{-100}$	$478 \pm 15^{+43}_{-24}$

(in MeV/c^2)

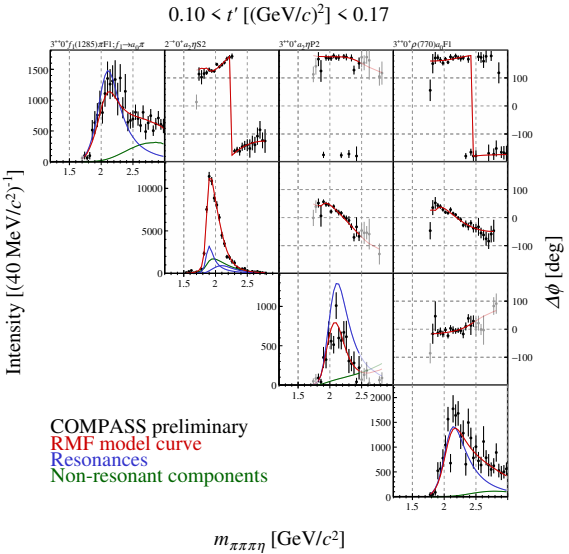

$K_S^0 K^-$

- $a_4(1970)$ consistent with previous measurements
- Second a_4 measured

	$K_S^0 K^-$
m_0	$1952.2 \pm 1.8^{+3.0}_{-3.5}$
Γ_0	$327 \pm 4^{+6}_{-6}$

(in MeV/c^2)

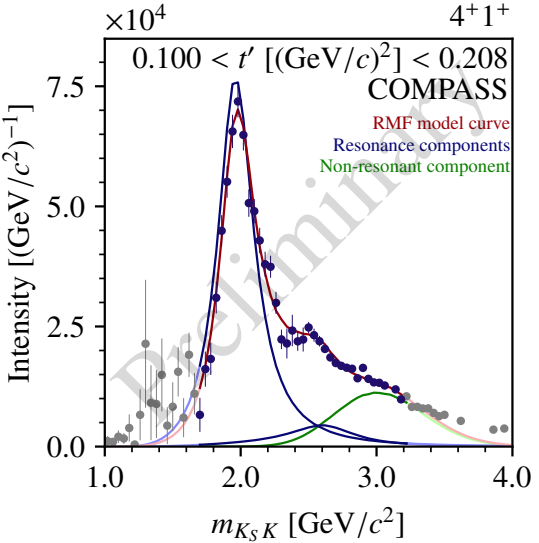

$\omega\pi^-\pi^0$

- 2 decay channels:
  $b_1(1235)\pi$& $\rho(770)\omega$
- $a_4(1970)$ consistent with previous measurements

	$K_S^0 K^-$	$\omega\pi\pi$
m_0	$1952.2 \pm 1.8^{+3.0}_{-3.5}$	$1973 \pm 3^{+15}_{-8}$
Γ_0	$327 \pm 4^{+6}_{-6}$	$311 \pm 8^{+10}_{-46}$

(in MeV/c^2)

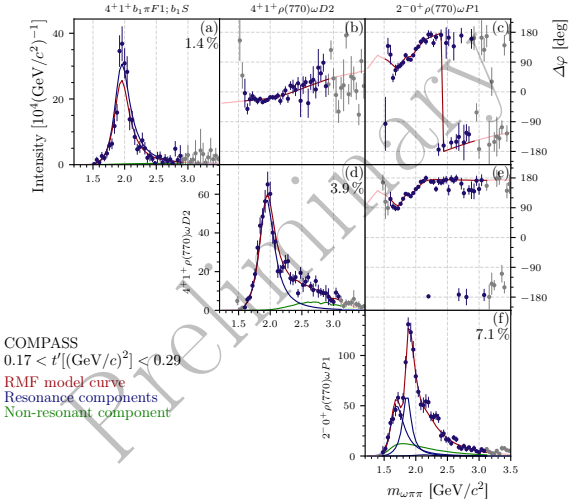

$\pi^-\pi^-\pi^+\eta$

- 1 decay channels:
  $f_1(1285)\pi$
- $a_4(1970)$ consistent with previous measurements

	$K_S^0 K^-$	$\omega\pi\pi$	$\pi^-\pi^-\pi^+\eta$
m_0	$1952.2 \pm 1.8^{+3.0}_{-3.5}$	$1973 \pm 3^{+15}_{-8}$	$2036 \pm 8^{+12}_{-69}$
Γ_0	$327 \pm 4^{+6}_{-6}$	$311 \pm 8^{+10}_{-46}$	$386 \pm 20^{+20}_{-93}$

(in MeV/c^2)

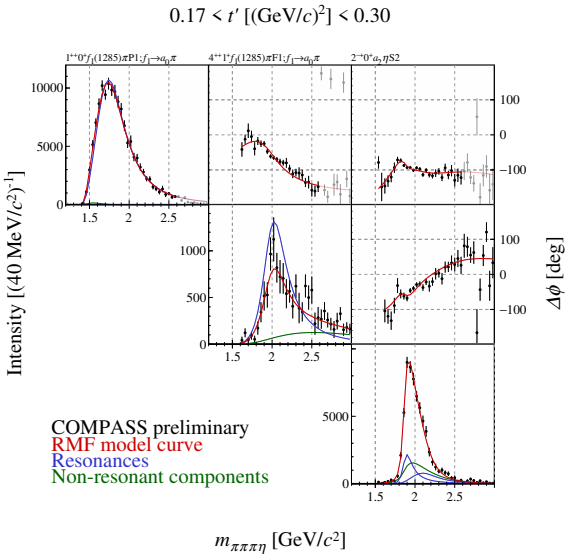

Details on $\pi\pi\pi\eta$ PWA

Isobar model (chain of two-body decays):

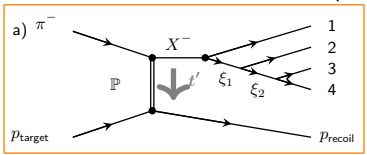

Example:

$$X \to (\pi\pi\eta)\,\pi, \quad (\pi\pi\eta) \to (\pi\eta)\pi, \quad (\pi\eta) \to \pi\,\eta$$

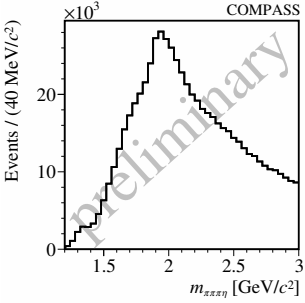

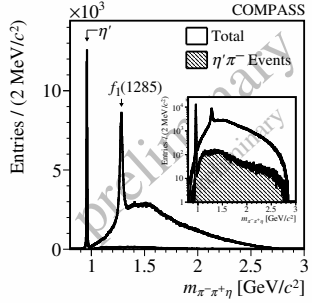

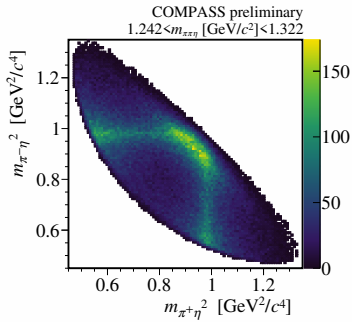

Isobar model for $\pi^-\pi^+\pi^-\eta$

Isobar model (chain of two-body decays):

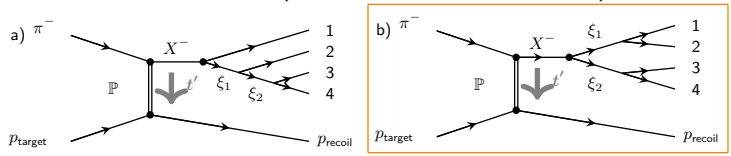

$$X \to (\pi\pi)(\pi\eta), \quad (\pi\pi) \to \pi\,\pi, \quad (\pi\eta) \to \pi\,\eta$$

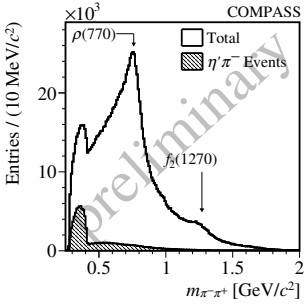

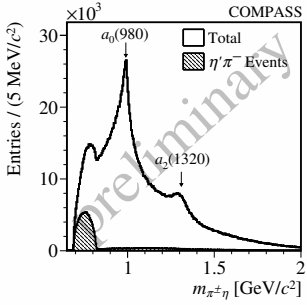

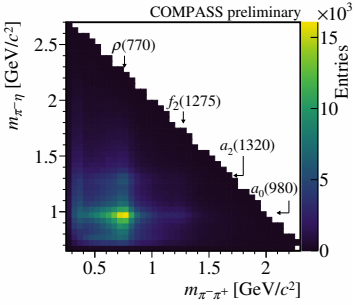

Strategy for wave-set selection per bin

- Truncation of partial-wave expansion needed

$$\mathcal{I}(\tau_i) = \left| \sum_a^{N_{\text{waves}}} \mathcal{T}_a \Psi_a(\tau_i) \right|^2$$

- 15 isobars and 18 decay channels
- Generate a wave pool with
  - 15 isobars and 18 decay channels
  - $J, L < 7$, $M < 2$, $\epsilon = +$
- Perform wave-set selection (WSS) fit:

$$\log(\mathcal{L}_{\text{WSS}}) = \log(\mathcal{L}_{\text{ext.}}) - \underbrace{\sum_a \log\left(1 + \frac{|\mathcal{T}_a|^2 \cdot I_{aa}}{\Gamma}\right)}_{\text{Cauchy regularization term}}$$

- Extract wave set and perform main fit

Wave selection by Cauchy regularization:

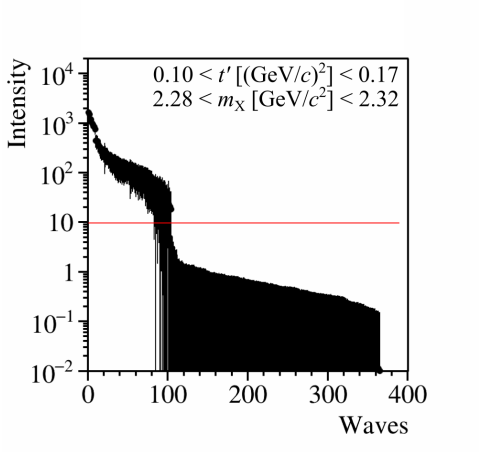

- Phenomenological Regge amplitude for Pomeron flux factor:

$$F_{\mathbb{P}p}\left(x_{\mathbb{P}}, t'\right) \propto \frac{e^{-b_{\mathbb{P}}t'}}{x_{\mathbb{P}}^{2\alpha_{\mathbb{P}}(t')-1}}, \text{ where } x_{\mathbb{P}} \approx \frac{m_X}{s} \text{ and } \alpha_{\mathbb{P}}\left(t'\right) = \alpha_0 - \alpha' t'$$

- Normalization and $e^{-b_{\mathbb{P}}t'}$ is absorbed in coupling parameters of resonance-model:

$$\left|\mathcal{P}_{\mathbb{P}}\left(m_X, t'\right)\right|^2 = \left(\frac{s}{m_X^2}\right)^{2\alpha_{\mathbb{P}}\left(t'\right)-1}.$$

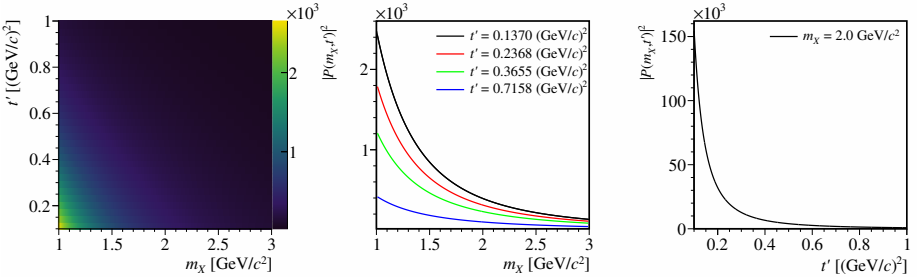

Consistency check of t'-dependence

Expectation for diffractive resonance production

- $\sigma\left(t'\right) \propto (t')^{M} \cdot \exp\left(-b \cdot t'\right)$
- Impact parameter picture: $b = \frac{R^2}{2}$

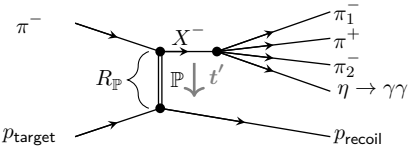

- For interaction ranges on the scale of the nucleon size: $b \approx 8\,(\text{GeV}/c)^{-2}$

$\rightarrow$ Fit integrated model for $\sigma\left(t'\right)$ to integrated signal components from RMF

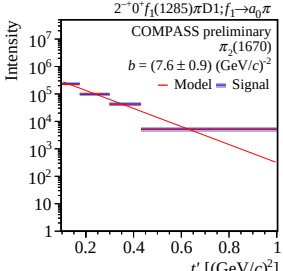

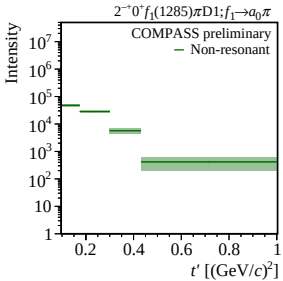

Consistency check of t'-dependence

Expectation for diffractive reson

- $\sigma\left(t'\right) \propto \left(t'\right)^{M} \cdot \exp\left(-b \cdot t'\right)$
- Impact parameter picture: $b =$

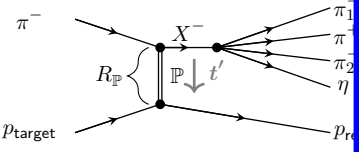

- For interaction ranges on the size: $b \approx 8\,(\text{GeV}/c)^{-2}$

$\rightarrow$ Fit integrated model for $\sigma\left(t'\right)$ components from RMF

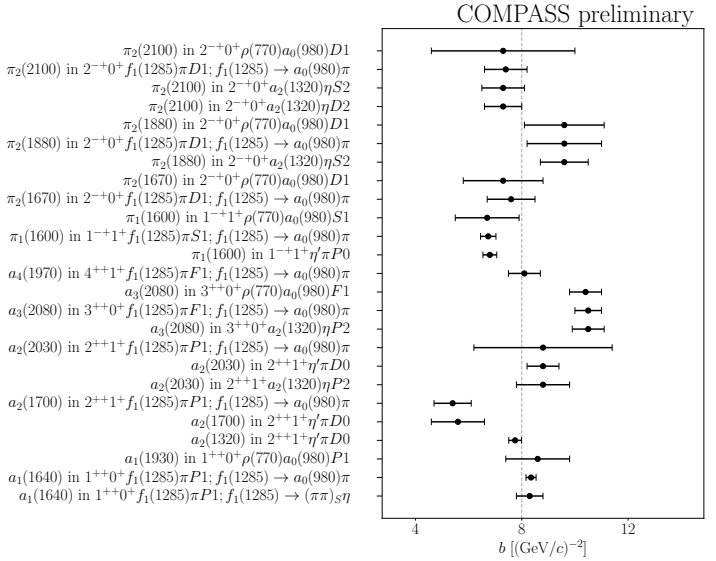

- **Reflectivity basis:** go into eigenbasis of reflection operator through production plane with eigenvalues $\varepsilon = \pm 1$ (reflectivity), accounting for spin projection of X:

$$ {}^{\varepsilon}Y_{\ell}^{m}(\Omega) \equiv \mathcal{N}_m \left[Y_{\ell}^{m}(\Omega) - \varepsilon\, P\, (-)^{\ell - m} Y_{\ell}^{-m}(\Omega) \right] \qquad \text{with} \qquad \mathcal{N}_m = \begin{cases} 1/\sqrt{2}, & m > 0, \\ 1/2, & m = 0, \\ 0, & m < 0. \end{cases} $$

  - Note: in reflectivity basis, $m \geq 0$
  - Amplitudes with opposite ε do not interfere:

$$ \mathcal{I}(\Omega) = \sum_{\varepsilon = \pm 1} \left| \sum_{\ell m}^{N_{\text{waves}}^{\varepsilon}} {}^{\varepsilon}\mathcal{T}_{\ell m}\, {}^{\varepsilon}Y_{\ell}^{m}(\Omega) \right|^2 = \sum_{\varepsilon = \pm 1} \sum_{\ell m} \sum_{\ell' m'} {}^{\varepsilon}Y_{\ell}^{m}(\Omega)\, {}^{\varepsilon}\varrho_{m m'}^{\ell \ell'}\, {}^{\varepsilon}Y_{\ell'}^{m'\,*}(\Omega) \qquad \text{with} $$

  - Just a basis change $\Longrightarrow$ physics remains unchanged

- **High-energy limit**
  - Reflectivity ε corresponds to naturality ($\eta = P(-1)^J$) of exchanged Reggeon
  - Pomeron exchange (natural parity) dominates $\Longrightarrow \varepsilon = +1$
  - Much less partial waves with $\varepsilon = -1$ than with $\varepsilon = +1$
    $\Longrightarrow$ reduces number of fit parameters

Comparison with results of BNL E852

- BNL E852 analysis of $\pi\pi\pi\eta$ with 10x less number of events
- Beam momentum at $18\,\mathrm{GeV}/c$
- No t'-dependence
- Only plots for three $f_1(1285)\pi^-$-wave published $\rightarrow$ Compare intensities and phases with new results from COMPASS
- Perform fit with reduced wave set to reveal artifacts

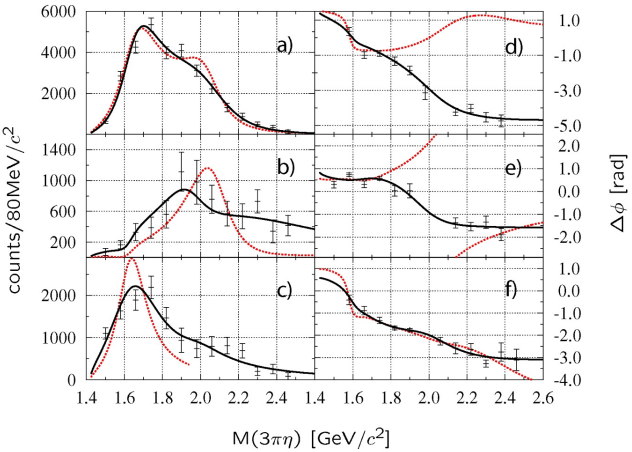

a)$1^{++}0^+f_1\pi P1$, b) $2^{-+}0^+f_1\pi D1$, c) $1^{-+}1^+f_1\pi S1$
[BNL E852, PLB, V595 109, 2004]

Comparison with results of BNL E852

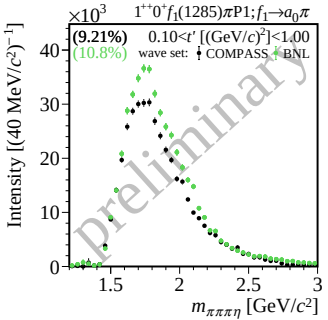

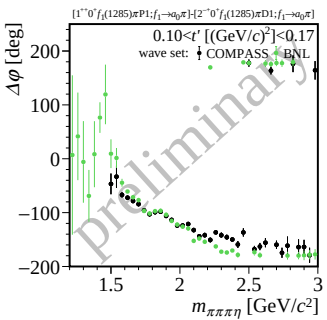

COMPASS data

- COMPASS wave set (290 waves)
- BNL E852 wave set (53 waves)

Comparison with results of BNL E852

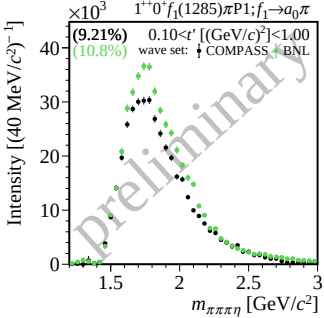

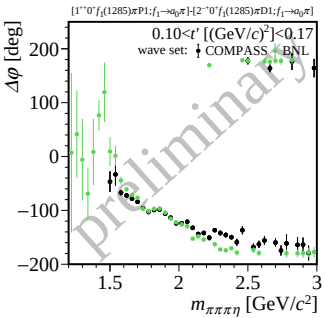

COMPASS data

- COMPASS wave set (290 waves)
- BNL E852 wave set (53 waves)

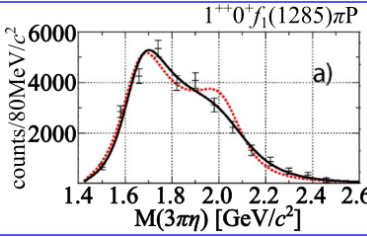

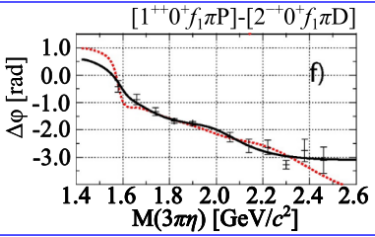

BNL E852 data

- Model 1 (main)
- Model 2

Comparison with results of BNL E852

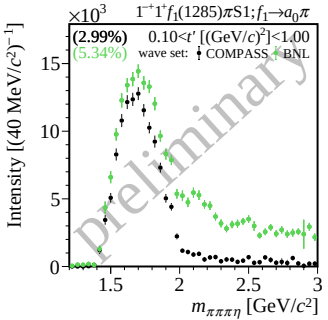

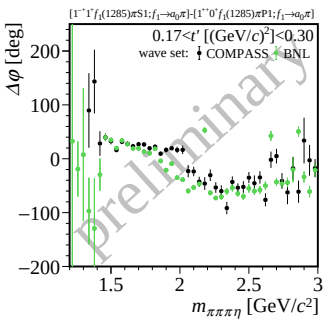

COMPASS data

- COMPASS wave set (290 waves)
- BNL E852 wave set (53 waves)

Comparison with results of BNL E852

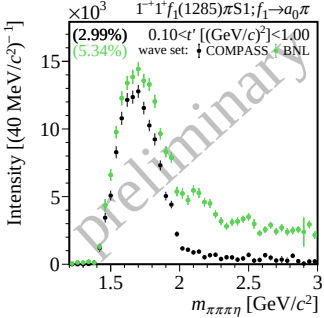

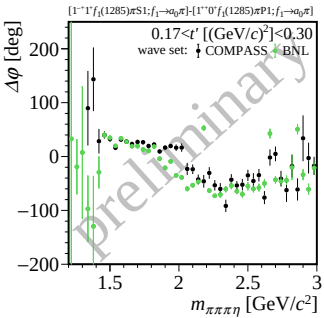

COMPASS data

- COMPASS wave set (290 waves)
- BNL E852 wave set (53 waves)

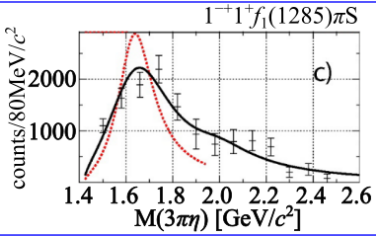

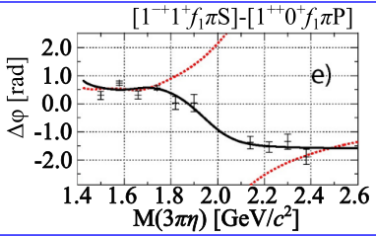

BNL E852 data

- Model 1 (main)
- Model 2

Used Isobars

sub-system	isobars	propagator term	parameter
$\pi^-\pi^+\eta$	$\eta'(957)$	real Double-Gaus	obtained from fit to data
	$f_1(1285)$	const. Breit-Wigner	$m_0 = 1281.4\,\mathrm{MeV/c^2}$, $\Gamma_0 = 22.0\,\mathrm{MeV/c^2}$
	$\eta(1295)$	const. Breit-Wigner	$m_0 = 1295.0\,\mathrm{MeV/c^2}$, $\Gamma_0 = 55.0\,\mathrm{MeV/c^2}$
	$f_1(1420)$	const. Breit-Wigner	$m_0 = 1426.0\,\mathrm{MeV/c^2}$, $\Gamma_0 = 54.0\,\mathrm{MeV/c^2}$
	$\rho(1450)$	const. Breit-Wigner	$m_0 = 1465.0\,\mathrm{MeV/c^2}$, $\Gamma_0 = 400.0\,\mathrm{MeV/c^2}$
$\pi^-\pi^+\pi^-$	$a_1^-(1260)$	Bowler	$m_0 = 1299.0\,\mathrm{MeV/c^2}$, $\Gamma_0 = 380.0\,\mathrm{MeV/c^2}$
	$a_2^-(1320)$	rel. Breit-Wigner	$m_0 = 1314.5\,\mathrm{MeV/c^2}$, $\Gamma_0 = 106.6\,\mathrm{MeV/c^2}$
	$\pi^-(1800)$	const. Breit-Wigner	$m_0 = 1804.0\,\mathrm{MeV/c^2}$, $\Gamma_0 = 220.0\,\mathrm{MeV/c^2}$
	$\pi_2^-(1670)$	const. Breit-Wigner	$m_0 = 1642\,\mathrm{MeV/c^2}$, $\Gamma_0 = 311\,\mathrm{MeV/c^2}$
$\pi\eta$	$a_0^\pm(980)$	Flatté	$m_0 = 987.4\,\mathrm{MeV/c^2}$, $\Gamma_0 = 75.0\,\mathrm{MeV/c^2}$ $r = 1.05$, $g_{\pi\eta} = 0.164$
	$a_2^-(1320)$	rel. Breit-Wigner	$m_0 = 1314.5\,\mathrm{MeV/c^2}$, $\Gamma_0 = 106.6\,\mathrm{MeV/c^2}$
$\pi^-\pi^+$	$(\pi^-\pi^+)_S$	J. Pelaez et al.	
	$\rho(770)$	rel. Breit-Wigner	$m_0 = 768.5\,\mathrm{MeV/c^2}$, $\Gamma_0 = 150.7\,\mathrm{MeV/c^2}$
	$f_0(980)$ (for $\pi(1800)$-decay)	Flatté	$m_0 = 980.0\,\mathrm{MeV/c^2}$ $r = 4.21$, $g_{\pi\pi} = 0.165$
	$f_2(1275)$	rel. Breit-Wigner	$m_0 = 1275.0\,\mathrm{MeV/c^2}$, $\Gamma_0 = 185.0\,\mathrm{MeV/c^2}$

counter	Primary Decay	Secondary Decay	Tertiary Decay	Topology
0	$X^- \to f_1(1285)\pi^-$	$f_1(1285) \to a_0^\pm(980)\pi$	$a_0^\pm(980) \to \pi^\pm\eta$	a
1	$X^- \to f_1(1285)\pi^-$	$f_1(1285) \to (\pi\pi)_S\eta$	$(\pi\pi)_S \to \pi^-\pi^+$	a
2	$X^- \to \eta(1295)\pi^-$	$\eta(1295) \to a_0^\pm(980)\pi$	$a_0^\pm(980) \to \pi^\pm\eta$	a
3	$X^- \to \eta(1295)\pi^-$	$\eta(1295) \to (\pi\pi)_S\eta$	$(\pi\pi)_S \to \pi^-\pi^+$	a
4	$X^- \to a_1^-(1260)\eta$	$a_1^-(1260) \to \rho(770)\pi$ (S-Wave)	$\rho(770) \to \pi^-\pi^+$	a
5	$X^- \to a_1^-(1260)\eta$	$a_1^-(1260) \to \rho(770)\pi$ (D-Wave)	$\rho(770) \to \pi^-\pi^+$	a
6	$X^- \to a_2^-(1320)\eta$	$a_2^-(1320) \to \rho(770)\pi$ (D-Wave)	$\rho(770) \to \pi^-\pi^+$	a
7	$X^- \to (\pi\pi)_S a_0^-(980)$	$(\pi\pi)_S \to \pi^-\pi^+$	$a_0^-(980) \to \pi^-\eta$	b
8	$X^- \to (\pi\pi)_S a_2^-(1320)$	$(\pi\pi)_S \to \pi^-\pi^+$	$a_2^-(1320) \to \pi^-\eta$	b
9	$X^- \to \rho(770)a_0^-(980)$	$\rho(770) \to \pi^-\pi^+$	$a_0^-(980) \to \pi^-\eta$	b
10	$X^- \to \rho(770)a_2^-(1320)$	$\rho(770) \to \pi^-\pi^+$	$a_2^-(1320) \to \pi^-\eta$	b
11	$X^- \to f_2(1275)a_0^-(980)$	$f_2(1275) \to \pi^-\pi^+$	$a_0^-(980) \to \pi^-\eta$	b
12	$X^- \to \eta'(957)\pi^-$	$\eta'(957) \to \pi^-\pi^+\eta$	-	c

counter	Primary Decay	Secondary Decay	Tertiary Decay	Topology
13	$X^- \to f_1(1420)\pi^-$	$f_1(1420) \to a_0^{\pm}(980)\pi$	$a_0^{\pm}(980) \to \pi^{\pm}\eta$	a
14	$X^- \to \rho(1450)\pi^-$	$\rho(1450) \to \rho\eta$ (P-Wave)	$\rho \to \pi^-\pi^+$	a
15	$X^- \to \pi^-(1800)\eta$	$\pi^-(1800) \to f_0(980)\pi^-$ (S-Wave)	$f_0(980) \to \pi\pi$	a
16	$X^- \to \pi_2^-(1670)\eta$	$\pi_2^-(1670) \to \rho\pi^-$ (F-Wave)	$\rho \to \pi\pi$	a
17	$X^- \to \pi_2^-(1670)\eta$	$\pi_2^-(1670) \to f_2(1275)\pi^-$ (S-Wave)	$f_2(1275) \to \pi\pi$	a

- Data split into bins of $(m_X,\, t')$ and use intensity function with $rank = 1$ and $\epsilon = +1$

$$I\left(\mathcal{T}_a, \mathcal{T}_b, \tau_i = \{\tau_1, \tau_2\}\right) = \underbrace{\left|\sum_a \mathcal{T}_a \Psi_a^{\text{sym.}}(\tau_i)\right|^2}_{\text{all waves but } \eta'\pi} + \underbrace{\left|\sum_b \mathcal{T}_b \Psi_b(\tau_1)\right|^2}_{\eta'\pi\text{-waves}} + \underbrace{\left|\sum_b \mathcal{T}_b \Psi_b(\tau_2)\right|^2}_{\eta'\pi\text{-waves}} + |\mathcal{T}_{\text{flat}}|^2$$

- Decay amp $\Psi^{\epsilon}_{a,b}$ are calculated from data using isobar model. Bose&Isospin sym.
- Anchor waves: $1^{++}0^+ f_1(1285)\pi^- P1, f_1(1285) \to a_0(980)\pi$ for a and $1^{-+}1^+\eta'\pi^- P1$ for b
- Production amplitudes $\mathcal{T}^{r,\epsilon}_{a,b}$ are determined by extended log-likelihood fit per $(m_X,\, t')$-bin
- Possible decay chains:
  - $X \to (\pi^-\pi^+\eta) + \pi^-$ (a)
  - $X \to (\pi^-\pi^+\pi^-) + \eta$ (a)
  - $X \to (\pi^-\pi^+) + (\pi^-\eta)$ (b)
  - $X \to \eta' + \pi^-$ (c)

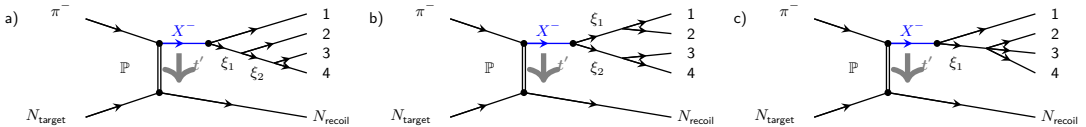

Weighted MC - $m_X < 3.0 GeV/c^2$

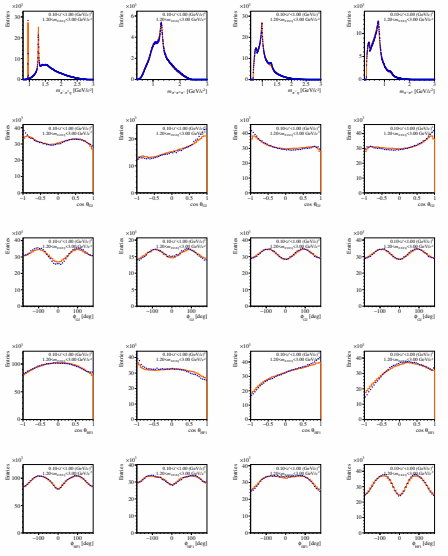

Weighted MC - $0.1\,\mathrm{GeV}^2/c^2 < t' < 0.3\,\mathrm{GeV}^2/c^2$

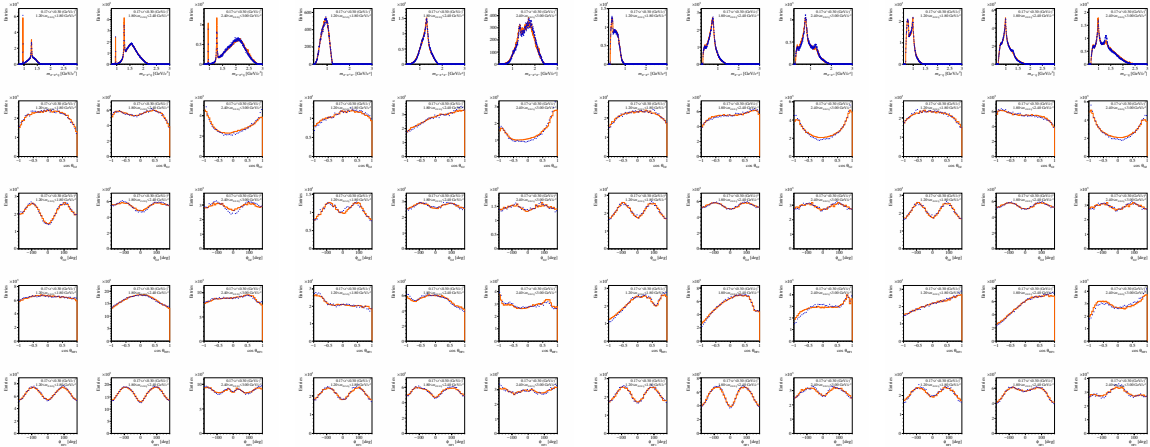

- **WASP** = **W**ave **A**nalysis **S**oftware **P**ackage

Predicted branching fractions

Hybrid meson in flux tube model

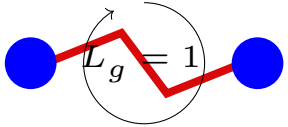

- $L = 1$ mesons are preferred
- Preferred channels: $b_1\pi, f_1\pi, a_1\pi$, ..

For a 1^{-+} hybrid at 1.6 GeV one has

	$b_1\pi$	$\rho\pi$	$f_1\pi$	$\eta(1295)\pi$	K^*K	
this work	24	9	5	2	.8	MeV
IKP model	59	8	14	1	.4	MeV

where both models predict $\eta\pi$, $\eta'\pi$, $\rho\omega$ and $f_2\pi$ to be 0

[Page, Swanson, Szczepaniak, PRD 59, (1999) 034016]

Lattice QCD

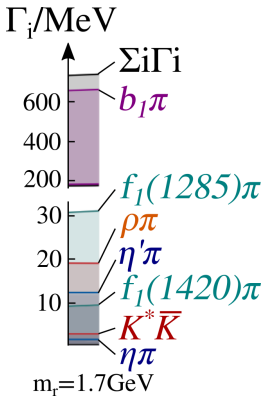

	Γ_i/MeV
$\eta\pi$	$0 \to 1$
$\rho\pi$	$0 \to 20$
$\eta'\pi$	$0 \to 12$
$b_1\pi$	$139 \to 529$
$K^*\bar{K}$	$0 \to 2$
$f_1(1285)\pi$	$0 \to 24$
$\rho\omega\left\{^1P_1\right\}$	$\lesssim 0.03$
$\rho\omega\left\{^3P_1\right\}$	$\lesssim 0.09$
$\rho\omega\left\{^5P_1\right\}$	$\lesssim 0.03$
$f_1(1420)\pi$	$0 \to 2$
$\Gamma = \sum_i \Gamma_i = 139 \to 590$	

[HadSpec, PRD 103, (2021) 054502]

Branching ratio of the $\pi_1(1600)$

The branching ratio for resonance j decaying into waves a and b can be estimated according to:

$$Br^j_{ab} \equiv \frac{\Gamma^j_a}{\Gamma^j_b} \text{ with } \Gamma^j_a = \sum_{t'} \mathcal{N}^j_a\left(t'\right) \text{ with}$$

$$\mathcal{N}^j_a\left(t'\right) = \left|\mathcal{C}^j_a\left(t'\right)\right|^2 \int_{m_{\min}}^{m_{\max}} \mathrm{d}m \; I_{aa}\left(m\right) \cdot m \cdot \left|\mathcal{D}^{\mathrm{R}}_j\left(m;\zeta^{\mathrm{R}}_j\right)\right|^2$$

with $m_{\mathsf{min}} = 1.2\ GeV/c^2$ and m_{max} =maximum of fit range.

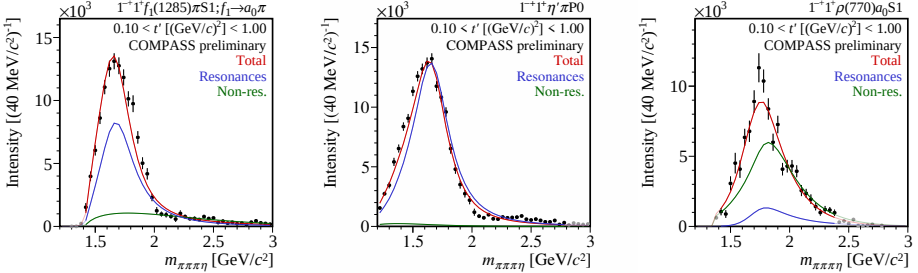

Branching ratio of the $\pi_1(1600)$

The branching ratio for resonance j decaying into waves a and b can be estimated according to:

$Br^j_{ab} \equiv \frac{\Gamma^j_a}{\Gamma^j_b}$ with $\Gamma^j_a = \sum_{t'} \mathcal{N}^j_a\left(t'\right)$ with

$$\mathcal{N}^j_a\left(t'\right) = \left|\mathcal{C}^j_a\left(t'\right)\right|^2 \int_{m_{\min}}^{m_{\max}} \mathrm{d}m \; I_{aa}\left(m\right) \cdot m \cdot \left|\mathcal{D}^{\mathrm{R}}_j\left(m;\zeta^{\mathrm{R}}_j\right)\right|^2$$

with $m_{\mathsf{min}} = 1.2\ GeV/c^2$ and m_{max} =maximum of fit range.

What can we measure and calculate?

$$\underbrace{\frac{\Gamma^{\pi_1(1600)}_{f_1(1285)\pi}}{\Gamma^{\pi_1(1600)}_{\eta'\pi}}}_{\text{reduced branching ratio}} = \underbrace{\frac{\Gamma^{\pi_1(1600)}_{f_1(1285)\pi;f_1\to a_0^{\pm}\pi^{\mp}\to\eta\pi^{\pm}\pi^{\mp}}}{\Gamma^{\pi_1(1600)}_{\eta'\pi;\eta'\to\pi^-\pi^+\eta}}}_{\text{measured branching ratio}} \cdot \underbrace{\frac{\Gamma^{\eta'}_{\pi^-\pi^+\eta}}{\Gamma^{f_1(1285)}_{a_0\pi\to\pi\pi\eta}}}_{\text{(PDG values)}} \cdot \underbrace{CG}_{\text{unobserved channels}}$$

Branching ratios of the $\pi_1(1600)$

Measured branching ratio (value $\pm \sigma_{\text{stat.}}$)

$$\frac{\Gamma^{\pi_1(1600)}_{f_1(1285)\pi;f_1\to a_0\pi;a_0\to\eta\pi}}{\Gamma^{\pi_1(1600)}_{\eta'\pi;\eta'\to\pi\pi\eta}} = 0.60 \pm 0.02$$

$$\frac{\Gamma^{\pi_1(1600)}_{f_1(1285)\pi;f_1\to a_0\pi;a_0\to\eta\pi}}{\Gamma^{\pi_1(1600)}_{\rho a_0(980);\rho\to\pi\pi;a_0\to\eta\pi}} = 4.47 \pm 0.50$$

$$\frac{\Gamma^{\pi_1(1600)}_{\rho a_0(980);\rho\to\pi\pi;a_0\to\eta\pi}}{\Gamma^{\pi_1(1600)}_{\eta'\pi;\eta'\to\pi\pi\eta}} = 0.13 \pm 0.02$$

Reduced Branching ratio (value $\pm \sigma_{\text{stat.}} \pm \sigma_{\text{PDG}}$)

$$\frac{\Gamma^{\pi_1(1600)}_{f_1(1285)\pi}}{\Gamma^{\pi_1(1600)}_{\eta'\pi}} = 1.01 \pm 0.034 \pm 0.107$$

$$\frac{\Gamma^{\pi_1(1600)}_{f_1(1285)\pi}}{\Gamma^{\pi_1(1600)}_{\rho a_0(980)}} = 12.4 \pm 1.4 \pm 6.3$$

$$\frac{\Gamma^{\pi_1(1600)}_{\rho a_0(980)}}{\Gamma^{\pi_1(1600)}_{\eta'\pi}} = 0.080 \pm 0.009 \pm 0.040$$

Branching ratios of the $\pi_1(1600)$

Measured branching ratio (value $\pm \sigma_{\text{stat.}}$)

$$\frac{\Gamma^{\pi_1(1600)}_{f_1(1285)\pi;f_1\to a_0\pi;a_0\to\eta\pi}}{\Gamma^{\pi_1(1600)}_{\eta'\pi;\eta'\to\pi\pi\eta}} = 0.60 \pm 0.02$$

$$\frac{\Gamma^{\pi_1(1600)}_{f_1(1285)\pi;f_1\to a_0\pi;a_0\to\eta\pi}}{\Gamma^{\pi_1(1600)}_{\rho a_0(980);\rho\to\pi\pi;a_0\to\eta\pi}} = 4.47 \pm 0.50$$

$$\frac{\Gamma^{\pi_1(1600)}_{\rho a_0(980);\rho\to\pi\pi;a_0\to\eta\pi}}{\Gamma^{\pi_1(1600)}_{\eta'\pi;\eta'\to\pi\pi\eta}} = 0.13 \pm 0.02$$

Reduced Branching ratio (value $\pm \sigma_{\text{stat.}} \pm \sigma_{\text{PDG}}$)

$$\frac{\Gamma^{\pi_1(1600)}_{f_1(1285)\pi}}{\Gamma^{\pi_1(1600)}_{\eta'\pi}} = 1.01 \pm 0.034 \pm 0.107$$

$$\frac{\Gamma^{\pi_1(1600)}_{f_1(1285)\pi}}{\Gamma^{\pi_1(1600)}_{\rho a_0(980)}} = 12.4 \pm 1.4 \pm 6.3$$

$$\frac{\Gamma^{\pi_1(1600)}_{\rho a_0(980)}}{\Gamma^{\pi_1(1600)}_{\eta'\pi}} = 0.080 \pm 0.009 \pm 0.040$$

Comparison to Exp. and Theory

- $\frac{\Gamma^{\pi_1(1600)}_{f_1(1285)\pi}}{\Gamma^{\pi_1(1600)}_{\eta'\pi}} = 1.1 \pm 0.3$ [VES, P.A.N. 68, (2005)]
- $\frac{\Gamma^{\pi_1(1600)}_{f_1(1285)\pi}}{\Gamma^{\pi_1(1600)}_{\eta'\pi}} = 3.80 \pm 0.78$ [E852, PLB 595, (2004)]
- LQCD: $\frac{\Gamma^{\pi_1(1600)}_{f_1(1285)\pi}}{\Gamma^{\pi_1(1600)}_{\eta'\pi}} \approx 2$
- Flux tube model: $\frac{\Gamma^{\pi_1(1600)}_{f_1(1285)\pi}}{\Gamma^{\pi_1(1600)}_{\eta'\pi}} \gg 1$

Freed isobar analysis

Freed Isobar Analysis

- In conventional analysis dynamical shape of isobars are fixed in decay amplitude
- Free the dynamics of the isobar and fit it with data:

$$\mathcal{I}(\tau_i) = \left| \sum_{a}^{N_{\text{waves}}} \sum_{k}^{N_{m_\xi \text{bins}}} \mathcal{T}_{a,k} \Psi'_{a,k}(\tau_i) \right|^2$$

with

$$\mathcal{T}_a \to \mathcal{T}_{a,k} = \mathcal{T}_a \mathfrak{T}_{a,k}$$

- The set $\mathfrak{T}_{a,k}$ describes the dynamics of the isobar in wave (a)

Results:

- Same result as conventional fit

→ Spin-exotic wave shows clear $\rho(770)$ signature

→ Supports assumptions of isobar model

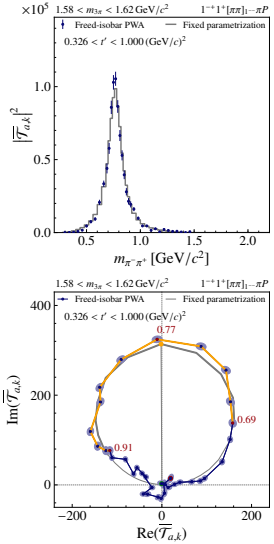

[COMPASS, PRD 105, 2022]

Goal: record 20 M $K^+\pi^-\pi^-$ events

- Beam line optimization (CERN North Area Consolidation)
  - Improved CEDAR efficiency: 85% $\rightarrow$ 95%
  - Beam intensity: 2.4 10^7 particles per spill $\rightarrow$ 7 10^7 particles per spill
- Reduced beam momentum:
  - Improved final-state PID efficiency: 50% $\rightarrow$ 81%

Luminosity for K with 40cm lH2 target: $\mathcal{L} = 1.24 \cdot 10^{30} cm^{-2} spill{-}1$

Cross section for diffractive production of $K\pi\pi$: $\sigma_{K\pi\pi} = 250\ \mu b$

$\Rightarrow$ 200 days with 3000 spills (4.8s) per day

$\Rightarrow$ we can record 20 M $K\pi\pi$ events in about 2 yrs

AMBER

Apparatus for Meson and Baryon Experimental Research